Cold Cratonic Roots and Thermal Blankets: How Continents Affect Mantle Convection

VALERY P. TRUBITSYN, WALTER D. MOONEY,[1]

United States Geological Survey, 345 Middlefield Rd., MS 977, Menlo Park, California 94025

AND DALLAS H. ABBOTT

Lamont-Doherty Earth Observatory, Palisades, New York 10964

Abstract

Two-dimensional convection models with moving continents show that continents profoundly affect the pattern of mantle convection. If the continents are wider than the wavelength of the convection cells (~3000 km, the thickness of the mantle), they cause neighboring deep mantle thermal upwellings to coalesce into a single focused upwelling. This focused upwelling zone will have a potential temperature anomaly of about 200°C, much higher than the 100°C temperature anomaly of upwelling zones generated beneath typical oceanic lithosphere. Extensive high-temperature melts (including flood basalts and late potassic granites) will be produced, and the excess temperature anomaly will induce continental uplift (as revealed in sea level changes) and the eventual breakup of the supercontinent. The mantle thermal anomaly will persist for several hundred million years after such a breakup. In contrast, small continental blocks (<1000 km diameter) do not induce focused mantle upwelling zones. Instead, small continental blocks are dragged to mantle downwelling zones, where they spend most of their time, and will migrate laterally with the downwelling. As a result of sitting over relatively cold mantle (downwellings), small continental blocks are favored to keep their cratonic roots. This may explain the long-term survival of small cratonic blocks (e.g., the Yilgarn and Pilbara cratons of western Australia, and the West African craton). The optimum size for long-term stability of a continental block is <3000 km. These results show that continents profoundly affect the pattern of mantle convection. These effects are illustrated in terms of the timing and history of supercontinent breakup, the production of high-temperature melts, and sea level changes. Such two-dimensional calculations can be further refined and tested by three-dimensional numerical simulations of mantle convection with moving continental and oceanic plates.

Introduction

ARCHEAN CRATONS have thick lithospheric roots and low heat flow (Grand and Helmberger, 1984; Pollack et al., 1993; Artemevia and Mooney, 2001). The preservation of Archean diamonds within these roots, as known from kimberlite eruptions, implies that they have had low heat flow and thick lithosphere since they formed (Richardson et al., 1984; Boyd et al., 1985; Nisbet, 1987). Indeed, the oldest model ages of cratonic roots are indistinguishable from the oldest ages of the overlying crust (Pearson et al., 1995), implying that Archean continents have experienced low heat flow since they formed.

In contradiction to these observations, some investigators have proposed that continents act as thermal blankets, i.e., low heat conduction through lithospheric roots causes the underlying asthenosphere to heat up (e.g., Anderson, 1989). This latter proposal is consistent with the development of superplumes that eventually break up supercontinents (Condie, 1998; White and McKenzie, 1995). Late-potassic granites within cratons also imply strong basal heating of the continental lithosphere (Campbell and Hill, 1988; Hill et al., 1992). Furthermore, if we consider Africa today, it is stationary with respect to the hot spot reference frame, and has an anomalously high topography relative to the other continents (Cogley, 1985). This anomalous elevation is consistent with the thermal blanket model: the African continental lithosphere is both heated and uplifted by a deep-seated mantle plume.

Thus, we seem to have two sets of contradictory observations. One set implies long-term cold continental roots and a second set implies hot continental roots. In this paper, we examine these apparently

[1]Corresponding author; email: mooney@usgs.gov

contradictory observations, and show that they can be reconciled if we allow the thermal history of continental blocks to depend on their lateral size. In so doing, we also show the profound affect that continents have on the pattern of mantle convection.

Properties of Mantle Convection

Five main properties of convection in the mantle are particularly relevant to this study: (1) the existence of cold, rigid continental lithosphere underlain by a warm, low-viscosity asthenosphere implies the existence of a large viscosity contrast (>3000 Pa-s) in the upper mantle; (2) regular, long-wavelength convection in the mantle, in combination with high-intensity, quasi-turbulent convection produces hot regions with varying shapes, such as diapirs, sheets, and ridges; (3) the olivine-perovskite mantle phase transition at a depth of 660 km is endothermic, and results in partial stratification of convection in the mantle (for example, some subducted plates continue to descend into the lower mantle, whereas others remain above the phase transition); (4) mantle material at the typical P-T conditions of oceanic lithosphere has a viscoplastic rheology that produces plate bending and the other mechanical behavior that we associate with plate tectonics; and (5) of particular importance to this study, the presence of continents above the convecting mantle profoundly affects the form of that convection; continental "thermal blankets" lead to regular and predictable patterns in the motions of both the convection system and the continents.

The first three properties were studied in great detail during the last three decades (e.g., see Schubert et al., 2001). Taking into account the fourth property leads to convection models that self-consistently describe the breakup of oceanic lithosphere into quasi-rigid plates (Tackley, 2000a, 2000b; Zhong et al., 2000). This paper investigates the fifth property of mantle convection. The effects of floating continents on mantle convection are important on time scales of more than 200 m.y., when continents behave like stable, rigid bodies, especially in comparison with the creation and subduction of oceanic lithospheric plates.

Previous Convection Models Incorporating Moving Continents

The role of moving oceanic plates and/or continents in mantle convection has been modeled using a numerical method that actually fixes mantle velocities rather than independently describing plate velocities (Olson and Corcos, 1980; Davies, 1986, 1988, 1989; Gurnis and Hager, 1988; Gable et al., 1991; King et al., 1992; Zhong and Gurnis, 1995; Doin et al., 1997). This approach can explain some aspects of plate movement, but could not be used to calculate plate velocities as an independent parameter.

A method for the self-consistent calculation of continental plate velocity within a convecting mantle was proposed by Gurnis (Gurnis, 1988; Gurnis and Zhong, 1991; Zhong and Gurnis, 1993, 1994). In this approach, a continent is considered as a highly viscous body floating in the mantle. Gurnis (1988) calculated the velocity of continents in his 2-D model by using a fixed marker point at the corner of each continent. This provided the first quantitative description of the assembly and dispersal of two continental blocks. Additional studies were presented by Gable et al. (1991), Lowman and Jarvis (1993, 1995, 1996), Bobrov et al. (1999), and Trubitsyn and Rykov (1995, 1998, 2000). The latter authors approximated continents as rigid bodies (as described by Euler's equations of motion), with viscous coupling to drive the plates (Trubitsyn, 2000). An iterative procedure was used to model convection, taking into account the rotation of continents and their mutual collisions. Oceanic plates were described by mantle convection equations incorporating a visco-plastic rheology (Tackley, 2000a; Zhong et al., 2000). These studies showed that the mantle under a fixed continent will become warmer, and that eventually hot upwelling zones arise, particularly under large continents. However, it was shown by Gurnis (1988), Trubitsyn and Rykov (1998), and Lowman and Jarvis (1996, 1999)—and will be demonstrated here—that the motions of continents produce additional effects on mantle evolution.

Input Parameters of Convection Models

Due to practical limitations on computational resources, it is not yet possible to make a numerical simulation of mantle convection that exactly matches the conditions in the real Earth. Our models do not match the real Earth in several aspects (Table 1). First, these models are two dimensional, while real convection is three dimensional. Second, these models use basal heating only, whereas both basal and internal heating drive real mantle convection. Third, our models use much lower Rayleigh numbers than the Rayleigh number

of actual terrestrial convection. Due to these limitations, for simplicity, we restrict our conclusions to those aspects of the modeling that are not strongly dependent on the numerical method used.

The Rayleigh number, Ra, defines the intensity of convection. For the present-day mantle it is high ($Ra_E \approx 10^7$) (Schubert et al., 2001). Thus, mantle convection is non-steady state and partially chaotic. However, chaotic behavior may obscure the main patterns of mantle convection that interest us. To avoid non-steady state effects that occur for high Rayleigh numbers ($Ra > 10^5$), we have made simple numerical models of mantle convection with variable viscosity for a Rayleigh number of $Ra_{ef} = 5 \cdot 10^4$. The effects of continents on mantle convection increase as the Rayleigh number is decreased, so our numerical results emphasize the pure effects of continents, and therefore provide simple and clear illustrations for tectonic analysis.

Whereas numerical simulations with a low Rayleigh number cannot represent the real Earth, such simulations illustrate many important properties of convection, as noted above. Furthermore, fully modeling the real Earth presents many technical challenges. For example, continents move together with rigid oceanic plates, which have profound effects. Conrad and Hager (2001) observed that cold, deeply subducting lithosphere strongly resists plate motion. Therefore, to model the real Earth at a high Rayleigh number we must also include the effects of surficial and subducted oceanic plates, presently an unsolved problem. Thus, a numerical model with a low effective Rayleigh number, as presented here, is a reasonable compromise that even has some advantages over a model with high Rayleigh number, but no oceanic plates.

Our simulations use the viscosity law:

$$\eta = \eta_0 \exp\left[(-4.6\,T + 0.92(1-z)\right],$$

where T is dimensionless temperature and z is the vertical coordinate. Thus, viscosity is modeled as temperature and pressure dependent. Temperature and pressure increases with depth cause viscosity changes of only 2 and 2.5 orders of magnitude, respectively.

The system of governing equations and boundary conditions for these 2-D numerical models are presented in Appendix A. We also show results for more realistic Rayleigh numbers that duplicate the general features of our low Rayleigh number calculations, but with much greater chaotic behavior in Appendix B.

TABLE 1. Input Parameters for Convection Modeling

System	Present Earth	Supercontinent	Small continent	Appendix
Rayleigh number (Ra)	1.00E+07	5.00E+04	5.00E+04	2.0E6
Heating	Basal + internal	Basal only	Basal only	Basal + internal
Viscosity law	Pressure, temperature and stress dependent[1]	$\eta = \eta_0\exp[(-4.6T + 0.92(1-z)]$	$\eta = \eta_0\exp[(-4.6T + 0.92(1-z)]$	$\eta = \eta_0\exp[(-4.6T + 0.92(1-z)]$
Convection pattern	Three-dimensional	Two-dimensional	Two-dimensional	Two-dimensional
Continent diameter, km	Variable	3000	300	3000?
Simulation duration, m.y.	3800	340?	1500?	500?
Phase boundary at 660 km	Yes	No	No	Yes
Number of cells	Variable	10	5	Variable

[1]See, for example, Forte and Mitrovica, 2000; Schubert et al., 2001.

Results: Convection with Two Continents that Combine to Form a Supercontinent

Continental assembly

Figure 1 (top) shows a simple 2-D convection system, with regularly spaced upwellings (red) and downwellings (green). Note that the lateral spacing between upwellings and downwelling is equal to the depth of the model, here 3000 km (the thickness of the mantle). Once mantle convection achieves a steady state, we introduce two free-floating continents to the system (Fig. 1; $t_1 = 0$ m.y.). The model input parameters are listed in Table 1. Our simulation starts with each continent on separate upwelling zones separated by a central downwelling zone. The continents then begin to move off the upwelling toward the central downwelling zone (Fig. 1; $t_2 = 4$ m.y.). At $t_3 = 15$ m.y. (Fig. 1C), the two continental blocks have just combined into a single supercontinent. Each continent moves a distance of ca. D/4 = 750 km over 15 m.y., a mean velocity of 5 cm/yr (extrapolated to Ra = 10^7). The downwelling zones remain intact and undisturbed until the two continents collide (Fig. 1; $t_3 = 15$ m.y.). The two continents are large enough to produce a combined continental block that is wider than the convection cells (3000 km). Thus, for our purposes, we define a supercontinent as any continental block with an average diameter of over 6000 km.

Mantle evolution under a supercontinent

Initially, the asthenosphere directly beneath the supercontinent gets colder (Fig. 2; $t_4 = 80$ m.y.), and thus the thickness of the cold thermal boundary layer beneath the new supercontinent increases. For simplicity, we take the initial temperature distribution in the two continents as being the same as in the oceanic lithosphere and mantle. This initial condition lets us show how temperature changes with the aging of the continents. The cooling of continental lithosphere and increasing thickness of the thermal boundary layer has been postulated to occur due to cooling by the ongoing subduction of oceanic plates on either side of a supercontinent (Schubert et al., 2001). However, despite this effect, we find the dominant factor is the thermal blanketing by the thick, low-conductivity continental lithosphere. Thus, the long-term thermal process beneath a supercontinent is the net heating of the mantle.

As the mantle beneath the supercontinent warms, it becomes lighter, forming a deep, low-pressure region. Because fluids move from regions of high pressure to regions of low pressure, the low pressure region causes thermal upwelling zones to migrate in the mantle toward the region beneath the center of the supercontinent (Fig. 2; $t_5 = 170$ m.y. and $t_6 = 200$ m.y.). The convection cells become narrower over time, until eventually the three upwelling zones merge into a single giant superplume (Fig. 2; $t_6 = 200$ m.y.).

The maximum temperature at the center of the superplume (Fig. 2; $t_6 = 200$ m.y.) is ~200°C higher than the maximum temperature at the center of an upwelling without continents (Fig. 1; $t_1 = 0$ m.y.). Thus, large continents result in the production of much hotter plumes.

Continental dispersal

After the supercontinent breaks up (Fig. 3; $t_7 = 220$ m.y. and $t_8 = 250$ m.y.), the area beneath what was previously the center of the supercontinent remains hot for several hundred million years (Fig. 3; $t_9 = 290$ m.y. and $t_{10} = 340$ m.y.). Thus, supercontinents have a long-lasting effect on the temperature regime within the upper mantle.

The state of the suboceanic mantle at $t_9 = 290$ m.y. resembles that in the present-day Atlantic, where the predicted reduced heat flow (i.e., the mantle heat flow) beneath the mid-oceanic region is six times greater than the reduced heat flow beneath continents (Gupta, 1993). This could explain why much of the Mid-Atlantic Ridge is a locus of hotspot volcanism (Fontigne and Schilling, 1996; Yu et al., 1997; Hanan et al., 2000).

Heating of the mantle beneath a supercontinent can generate dynamic topography. Comparing the elevation of the continents during the whole Wilson cycle, as simulated in Figures 1, 2, and 3, we see that continents are tilted, with one edge standing high from ca. 50 m.y. before break-up until 50 m.y. after breakup. Conversely, continental elevations are low when the continent sits over a mantle downwelling. Thus, one edge of each continental block should have been relatively high for ~100 m.y. before and after the breakup of Pangea and Rodinia. This prediction agrees with low sea level curves (Vail and Mitchum, 1979; c.f., discussion by Trubitsyn, 2000).[2]

---

[2] We note that an additional, opposing factor not considered here is the expected rise in sea level during supercontinent breakup due to creation of a larger volume of oceanic spreading ridges.
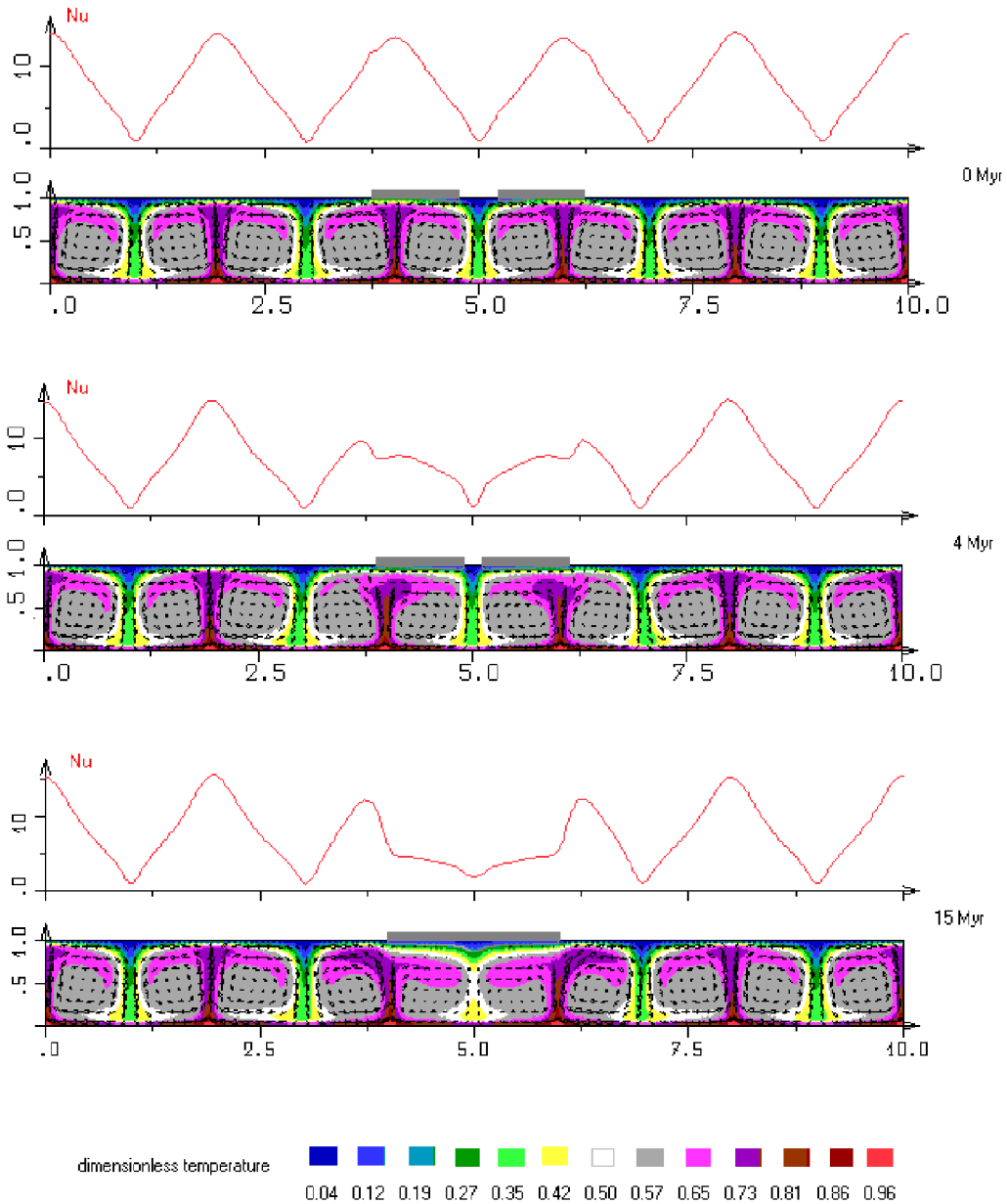
FIG. 1. Three time steps (0, 4, and 15 m.y.) illustrating the influence of two continents on the convecting mantle. Model parameters are from Table 1; governing equations are from Appendix A. Colors depict dimensionless subadiabatic (potential) temperature, from 1 to 0. Length of arrows is proportional to mantle velocities. The longest arrows equal a mantle velocity of roughly 10 cm/y. The red line above each picture shows the calculated distribution of surface dimensionless heat flow, i.e. the Nusselt number, Nu (x). The time of each simulation in m.y. is shown on the right side. At 0 m.y. two continents are instantaneously placed in the steady-state convecting mantle. At 4 m.y. the continents have moved away from the pink upwellings and approach each other above a green downwelling. At 15 m.y. the continents have formed a "supercontinent" where previously a cold downwelling existed. Note that the supercontinent (15 m.y.) has disturbed the initial steady-state convection (0 m.y.).

Figure 4 shows continental velocities during the Wilson cycle. Note that we do not know exactly how long it takes for two colliding continents to merge into a supercontinent. Also, our model does not include a calculation of the critical stresses that are required to break up a supercontinent. Figure 4 shows that their relative velocities are two times less than the typical mantle convection velocity of 10 cm/yr. Continental velocity is nearly zero during two time periods: t = 15–200 and t > 340 m.y.
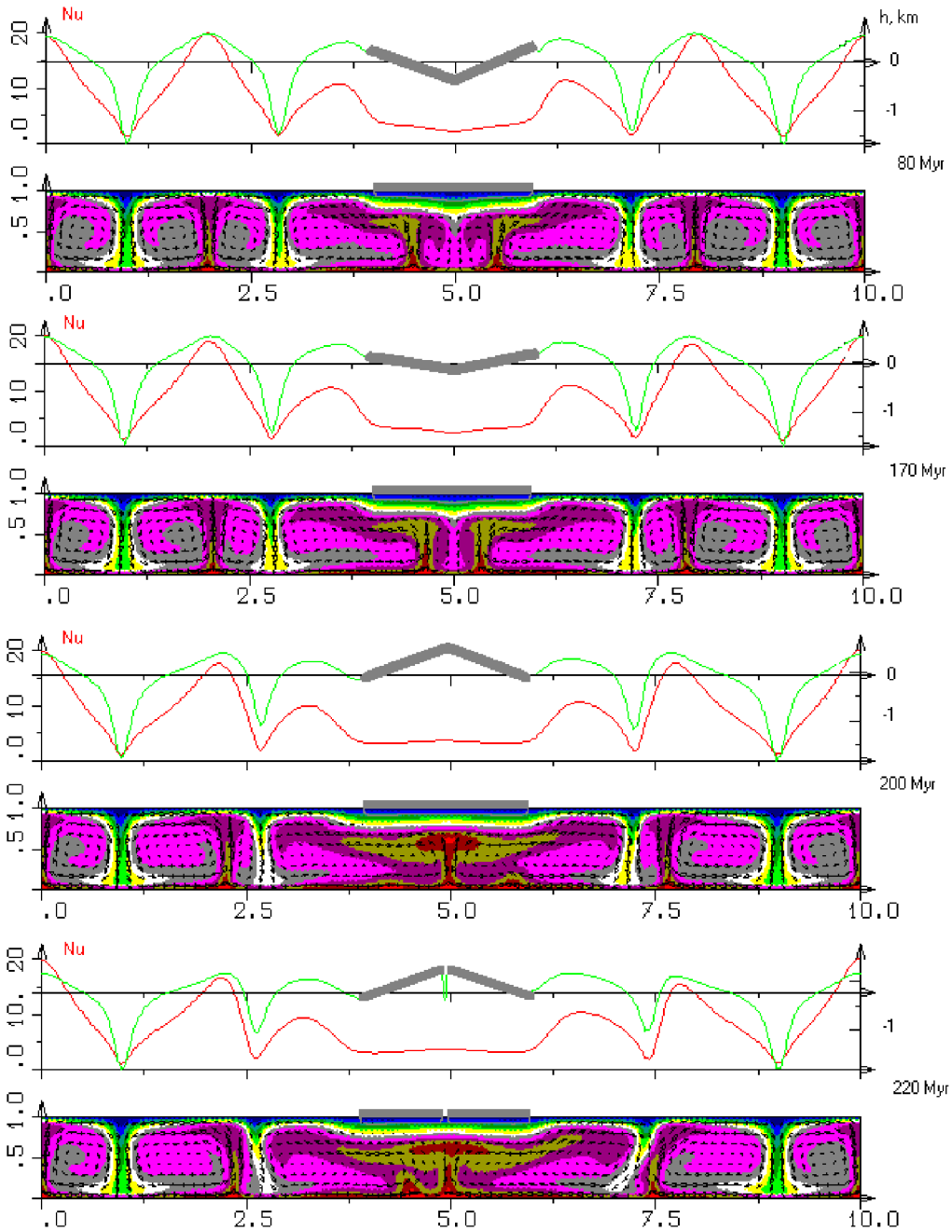
FIG. 2. Further evolution of the convection system in Figure 1. The green line above each picture is the topography (in km) of the surface of the model. At 80 m.y. the supercontinent is depressed by the last vestiges of the downwelling. At 170 m.y. two small upwellings (brown) begin to migrate to the center of the supercontinent. At 200 m.y. these upwellings have merged, and the supercontinent has positive topography. At 220 m.y. the initial rifting of the supercontinent has begun due to vigorous upwelling beneath the supercontinent.

Convection with a Small Continent

In this numerical simulation (Figure 5, Table 1), each convection cell has nearly the same width and the same height and there are few changes with time. Next we introduce a small free-floating continent into the system (Fig. 5; $t_1 = 0$ m.y.). The conti-

nent is just 300 km wide (0.1 of the mantle depth). The thickness of the continental block is 0.05 of the thickness of mantle, i.e. 150 km. At the start of our simulation, the continent is between an upwelling and a downwelling zone. The continent moves from the upwelling zone toward a downwelling (Fig. 5; $t_2 = 50$ m.y.). During this time, the continent has moved
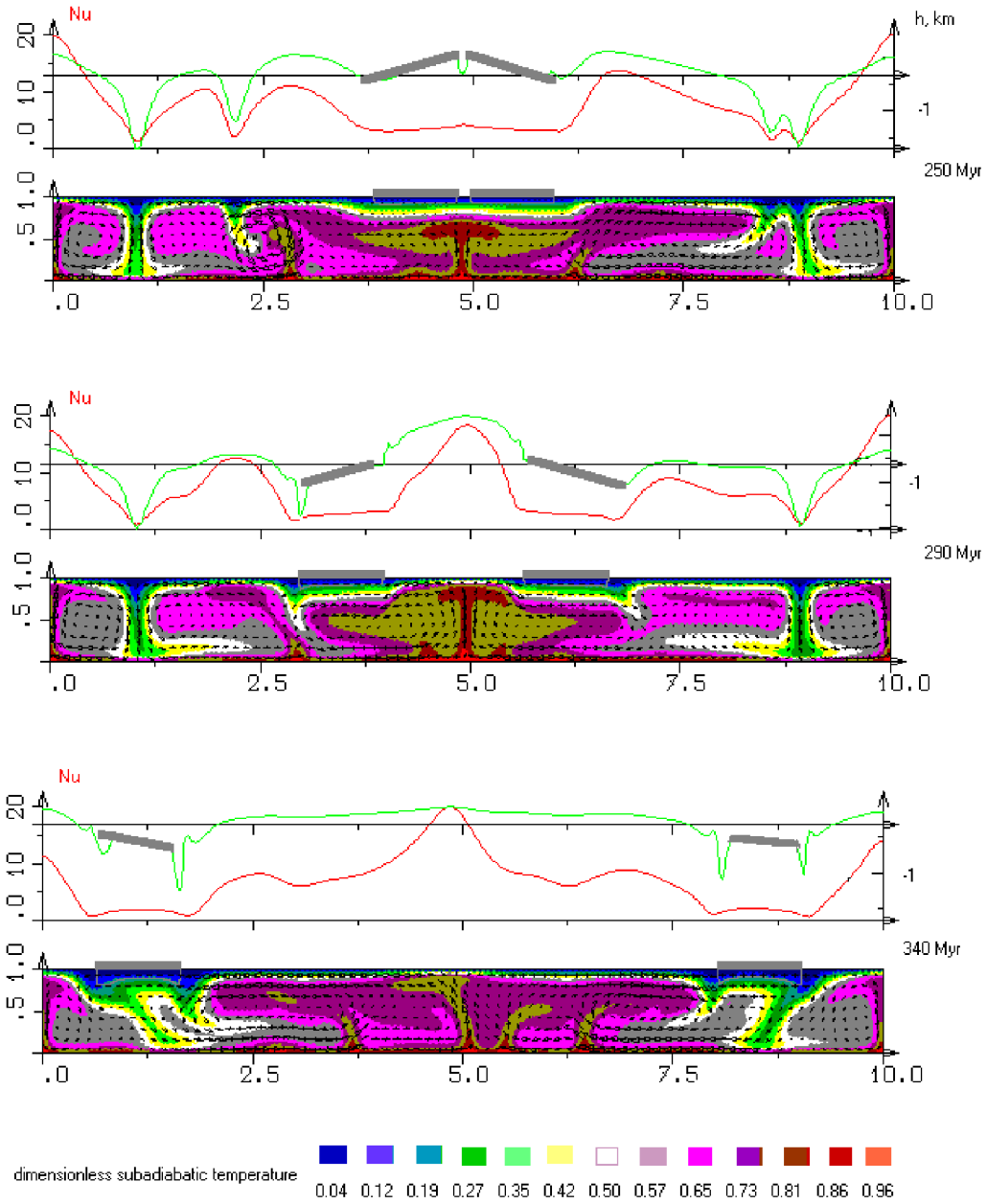
FIG. 3. Further evolution of the convection system in Figures 1 and 2. These three diagrams document the stages of continental dispersal. At 250 m.y. the continents continue to move apart, and have uplifted rift shoulders, much like the region bordering the present-day Red Sea. At 290 m.y. the continents have moved far apart, but the superplume continues to be active where the supercontinent had been (x = 5.0). The far edges of the continents have encountered downwellings and are tilted in sympathy. At 340 m.y. the continents are far apart and sit above strong downwellings, where they are depressed by 200–300 m.

about 1000 km. Thus its mean velocity is 2 cm/yr, less than half the mantle velocity.

Once this small continent arrives at the downwelling zone, it remains there for most of the remaining time. At $t_3 = 200$ m.y. (Fig. 5), the continent has already spent 150 m.y. at the downwelling. The presence of the continent only produces a small change in the left-hand upwelling, generating a feature that looks like a small plume. Further calculation shows that this plume has an insignificant effect on the continent. Only after about 1 G.y. (Fig. 5) do upwellings begin to move along the base of the model to a position beneath the continent. Further calculation shows that these upwellings are not large
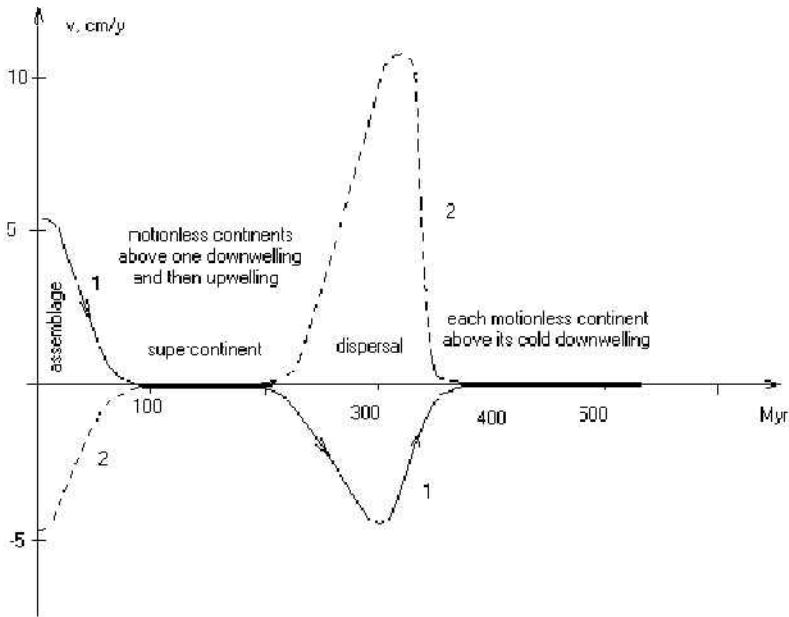
FIG. 4. Calculated velocities for both continents (v, cm/y) after extrapolation to Ra = 10^7. A solid line is used to represent continent 1, and a dashed line continent 2. The cycle from supercontinent formation to full dispersal requires 300 m.y.

enough to push the continent away from the downwelling. Thus, a downwelling essentially traps small continents in place (Fig. 5; t_1 = 0 yr, t_5 = 1.5 G.y.).

Mantle convection in the real Earth, which has a larger Rayleigh number, is nonsteady and chaotic (Schubert et al., 2001). As a result, the convection cells change their size over time. Therefore, even a small continent caught by a downwelling will not be fixed in space. It will migrate along with the downwelling.

In the case where many small continents are present (as would be true for most if not all of the Earth's history), there can be additional effects. Each small continent quickly (in ca. 10–50 m.y.) moves to a downwelling. If the number of continents is greater than the number of downwellings, two or three small continents go to one downwelling, collide, and coalesce to form a larger continent. When the lateral extent of this larger continent is comparable to the width of the convection cells (~3000 km), the supercontinent begins to act as a thermal blanket to convection and is able to leave the downwelling.

A continent with a diameter close to the mantle thickness (3000 km) spends roughly one-third of its time on a downwelling, one-third of its time as a part of a supercontinent on an upwelling, and one-third of its time moving between downwellings and

upwellings. Our model shows that, without additional external forcing, a small continent with a diameter of about 300 km cannot leave its downwelling for at least 1 G.y. This cold state of a small continent (in parallel with buoyancy and rheology) prevents continental lithosphere from mixing into the mantle and preserves lithospheric roots.

Discussion: Geological Implications of Modeling Results

In both numerical simulations presented here, continents produce significant changes in the morphology of upwelling and downwelling zones. Downwelling zones deviate from their former vertical geometry when continents approach and partially cover them. This suction effect of continents on subduction zones has been noted before (e.g., Uyeda, 1982), and results in the familiar dipping subduction zone. This is well defined by deep seismicity and seismic tomography.

Likewise, upwelling zones that move beneath continents also lose their highly regular geometry, and become much wider near their tops. When a supercontinent is present, the upper parts of the upwelling zones form the classic bulbous shape that was produced experimentally by Campbell and Griffiths (1989). This geometry of plume heads is
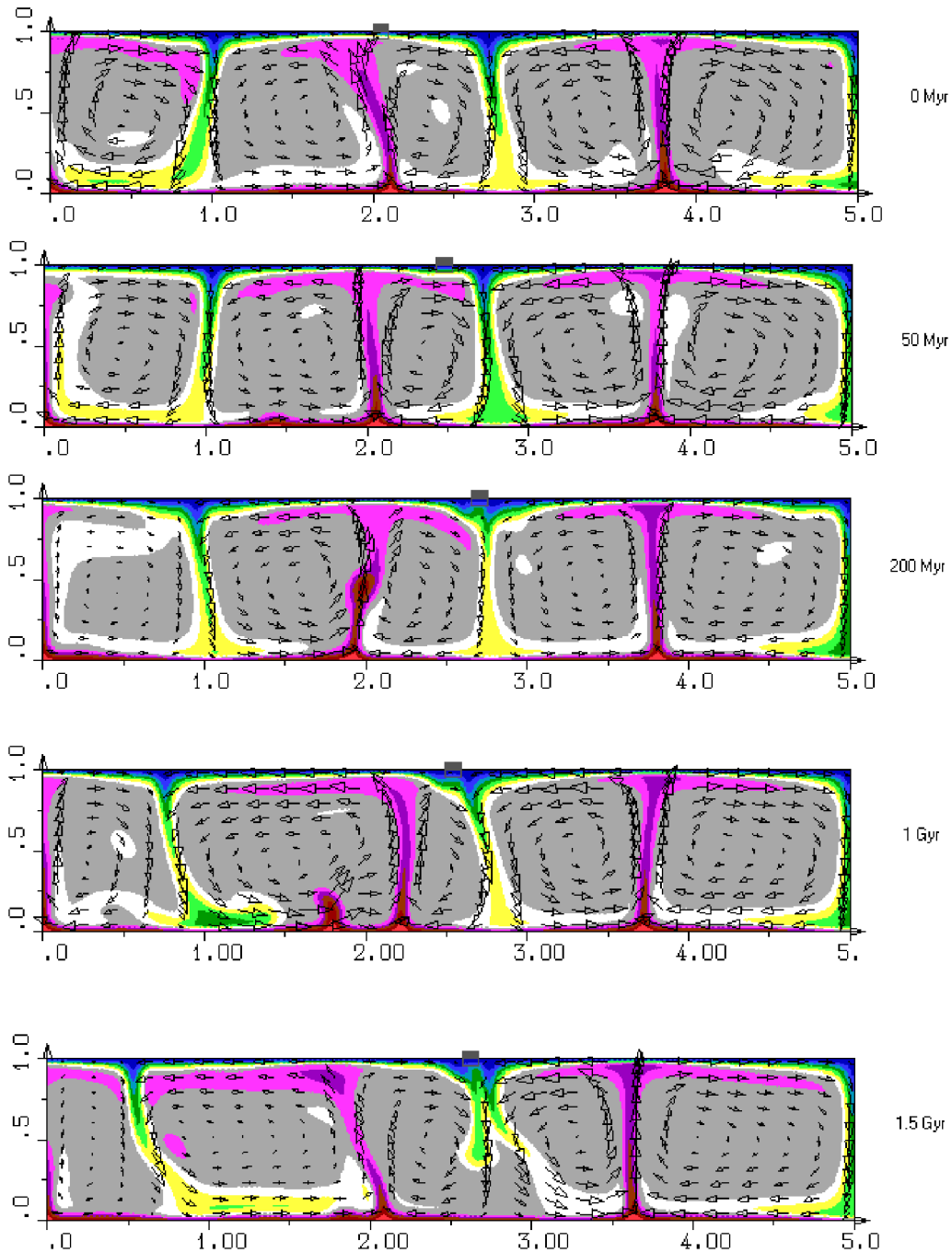
FIG. 5. Evolution of mantle convection with the presence of a small continent (length l = 300 km, thickness d = 150 km) and for $Ra_{ef} = 5 \cdot 10^5$ in an elongated box with five convection cells. The colors depict dimensionless subadiabatic (potential) temperature, from 1 to 0. Length of arrows is proportional to mantle velocities. The longest arrows equal a mantle velocity of ca. 7 cm/y (after extrapolation to $Ra = 10^7$). At 0 m.y. the continent moves to the right, away from the upwelling (pink). At 200 m.y. the continent is caught by the downwelling (green). From 200 m.y. to 1.5 G.y. the continent remains with the downwelling, but the convection system continues to evolve and does not reach steady state. Thus even a small continent affects the pattern of convection.

confined to supercontinents and does not occur beneath a small continent. The interior of the plume head has the highest temperatures and is the most likely source for high-T komatiitic lavas.

These 2-D numerical models are consistent with earlier suggestions that continents can act as thermal blankets. However, effective thermal blanketing is a function of continental size. We estimate the

TABLE 2. Diameter Calculated for Circular Archean Cratonic Blocks as Amalgamated by 1.6-1.8 G.y.[1]

Archean core	Surface area, km²	Diameter, km
North America	8.85E + 06	3356.05
East Antarctica	5.81E + 06	2718.90
Kaapvaal-Rhodesia	1.45E + 06	1358.608
Pilbara + Yilgarn	1.51E + 06	1384.968
East European Platform	1.88E + 06	1545.303
Siberia	3.72E + 06	2175.623
India	1.96E + 06	1580.94
Central Africa	5.8E6	2723.863
Amazon	1.34E6	1306.925

[1]Data from Abbott and Menke, 1990; Stoddard and Abbott, 1996.

TABLE 3. Diameter Calculated for Circular Continental Blocks[1]

Continent	Surface area, km²	Diameter, km
North America	2.34E + 07	5459
Antarctica	1.07E + 07	3688
Arabia	3.97E + 06	2247
Australia	7.49E + 06	3088
Eurasia	3.91E + 07	7052
India	4.31E + 06	2342
Africa	2.15E + 07	5233
South America	1.10E + 07	3740

[1]Data from Stoddard and Abbott, 1996.

threshold size to be equal to the thickness of the mantle (3000 km). When we compare this threshold size to the size of cratonic blocks, we see that the average diameter of the largest preserved cratonic blocks is 1500 to 3350 km (Table 2). Only one Archean cratonic block, that of North America, has a diameter larger than 3000 km. The maximum diameter of the Archean of North America (3356 km) is very similar to our estimated threshold diameter (3000 km) of non-supercontinental cratonic blocks. Larger cratonic blocks are more likely to be rifted, and thus reduced in size.

Several continents (i.e., including portions younger than the Archean) have diameters ≥3000 km (Table 3). We note that all but one of the continental blocks with diameters exceeding 3100 km (Table 3) contain one or more Cenozoic continental rifts. North America contains the Basin and Range Province. Antarctica has the East Antarctic rift zone. Africa is cut by the East African rift zone, and Eurasia, which has a radius of more than twice 3000 km, has two prominent Cenozoic rifts—the Baikal rift and the extensive Western European rift system. Only South America appears to violate this precept (the Amazon rift and the rift-related Parana basin are pre-Cenozoic and are not considered here). However, the geometry of South America is elongated north to south such that it may fit above a

single convection cell. In contrast to the examples cited above, none of the three smaller continental blocks (average radius <3100 km) has an internal rift.

Inasmuch as modeling suggests that a supercontinent sweeps together the mantle convection cells beneath, this implies that the magnitude of the temperature anomaly beneath a supercontinent is a function of its average diameter. The biggest supercontinents should produce the largest thermal anomalies and the highest degrees of partial melts. This inference seems to be borne out in the case of Pangea, which produced the largest known flood basalt province (Abbott and Isley, 2002) and is the largest known supercontinental block of the Phanerozoic (Marzoli et al., 1999).

These models suggest that the hottest mantle melts are preferentially produced beneath supercontinents and rifted oceanic basins formed during their breakup. The widest feeder dikes are produced by the largest plumes, and field evidence from such dikes suggest that there were many Precambrian supercontinents the size of Pangea or larger. Abbott and Isley (2002) estimated that there were six plume events in the Archean and Early Proterozoic, each at least 10 times as large as the Pangean superplume. Although a few of these plume events have a geochronology that might be coincident, there were at least four separate plume events 10 times as large as the Pangean superplume. Could each of these four massive plume events represent the legacy of a supercontinent that was significantly larger than Pangea? A combination of precise geochronology and paleomagnetic data will be required to test these ideas.

Late potassic granites are postulated to form as the result of a long-lived (100 m.y.) thermal anomaly in the underlying mantle (Campbell and Hill, 1988). The long residence times of supercontinents over downwellings suggests that such potassic granites were formed when that continent was part of a supercontinent. This hypothesis is consistent with another observation, that late potassic granites almost invariably follow a period of consolidation of smaller cratonic blocks into a larger cratonic block. Late potassic granites tend to be a mark of cratonization, in that the craton tends to undergo no significant internal deformation after this event.

If late potassic granites do reflect widespread heating of the base of the cratonic lithosphere by a supercontinent-induced plume, they may also be markers for another event. The mechanism for the formation of cratonic roots is still debated, but it is agreed that cratonic roots are very refractory and rigid. It has been suggested that recent continental superplume events have resulted in the addition of material to the base of the craton in South America (VanDecar et al., 1995). If this also occurred during the Archean, some cratonic roots may be composed of refractory mantle residues resulting from the extraction of superhot plume lavas during a supercontinental epoch. This model can be tested by looking at the degree of stratification by Mg number of cratonic roots in areas with late potassic granites. It can also be tested by comparing the ages of these stratified roots to the ages of the potassic granites. Because the thermal pulse will take a long time to travel through the lithosphere to the base of the crust, the base of the cratonic root should be tens of millions of years older than the age of the late potassic granites (Campbell and Hill, 1988; Hill et al., 1992). The base of the cratonic root should also have the same age as the region intruded by the late potassic granites.

Conclusions

We used very simple 2-D numerical simulations with low Rayleigh numbers to reveal the affects of continents on mantle convection. These models do not take into account non-steady state nor spherical effects, as described by Schubert et al. (2001). However, the models illustrate important qualitative effects, and provide a guide for interpreting observed geological data. These simulations show that mantle convection is significantly affected by drifting continents. Large continents (>3000 km in diameter) are highly effective as thermal blankets, and cause the underlying mantle to heat up. This thermal blanketing produces a low-pressure zone within the mantle that sweeps together thermal upwellings beneath the continent into a superplume. As a result, supercontinents generate the forces for their own dispersal by rifting. Large (~1 km) dynamic topography is also produced by hot, buoyant mantle upwellings, as are extensive high-temperature mantle melts.

Smaller continents (<1000 km in diameter) are too small to sweep up thermal convection cells. Instead, smaller continents tend to migrate toward downwelling zones and to remain there. Smaller continents develop thermal boundary layers that are too thick to be thermally eroded when the block is over an upwelling zone.

Many factors prevent mixing of the cratonic lithosphere into the mantle (Lenardic and Kaula, 1995; Lenardic, 1997, 1998; Moresi and Lenardic, 1997). They are as follows: high viscosity, chemical buoyancy, and viscoplastic rheology. We have only studied the evolution of the thermal state of floating continents, not the evolution of their buoyancy and rheology. Because the viscous forces of mantle flow tend to permanently drag smaller continents to the coldest downwellings, a small continent spends most of its time in a relatively cold state. Therefore, the viscosity of continental roots of small cratons remains relatively high.

Our results and those of previous papers (Gurnis, 1988; Gurnis and Zhong, 1991; Zhong and Gurnis, 1993, 1994; Trubitsyn and Rykov, 1995, 1998, 2000; Bobrov et al., 1999; Lowman and Jarvis, 1966, 1999; Trubitsyn, 2000) indicate that the mantle-continent convection system has two quasi-steady states, during which continents are motionless. In the first state, the continents are assembled into a supercontinent, and in the second state each continent occupies its own downwelling. During the Earth's history, the mantle-continent system has oscillated between these two states. On average, the continents assemble and disperse every 500–800 Ma.

Continents also affect the shape of mantle upwelling and downwelling zones. Beneath supercontinents, the shape of an upwelling zone just before continental breakup resembles the classic bulbous shape that is attributed to plume heads. Downwelling zones deviate from the vertical and become more narrow at the edge of continents, and are sucked beneath the continent by the low-pressure zone that they generate. Thus, the low subduction angles of some Benioff zones are partly due to the presence of continental blocks.

Continents play a major role in influencing the pattern of convection in the Earth. These simple simulations illustrate in two dimensions some of the important aspects of this role. Likewise, changes in mantle convection can induce the uplift, rifting, and dispersal of a supercontinent, as well as generate high-temperature melts, all processes that are preserved in the geologic record.

We do not present a model of convection in the real Earth. The main defects of our model are that: (1) a 2-D Cartesian model cannot describe cylindrical plumes; (2) use of a low Rayleigh number in the model suppresses secondary convection beneath plates, effects that were considered by Solomatov and Moresi (2000); and (3) the effects of highly viscous oceanic lithosphere, which are very important for mantle convection, are not included. Extending these numerical simulations to three dimensions, increasing the Rayleigh number, and including the effects of oceanic lithosphere holds the promise of providing a deeper understanding of the interplay between mantle convection and the evolution of the continents.

REFERENCES

Abbott, D. H., and Isley, A. E., 2002, The intensity, occurrence, and duration of superplume events and eras over geological time: Journal of Geodynamics, v. 34, p. 365–387.

Abbott, D. H., and Menke, W. H., 1990, The length of the global plate boundary at 2.4 Ga: Geology, v. 18, p. 58–65.

Anderson, D. L., 1989, Theory of the Earth: Boston, MA, Blackwell Scientific Publishers, 366 p.

Artemieva, I. M., and Mooney, W. D., 2001, Thermal thickness and evolution of Precambrian lithosphere: A global study: Journal of Geophysical Research, v. 106, p. 16,387–16,414.

Blankenbach, B., Busse, F., Christensen, U., Czerepes, L., Gunkel, D., Hansen, U., Jarvis, G., Koch, M., Marquatt, G., Moore, D., Olson, P., Schmeling, H., and Schnaubelt, T., 1989, A benchmark comparison for convection codes: Geophysical Journal International, v. 98, p. 23–38.

Bobrov, A. M., Jacoby, W., and Trubitsyn, V. P., 1999, Effects of Rayleigh number, length, and thickness of continent on time of mantle flow reversal: Journal of Geodynamics, 27, 133–145.

Boyd, F. R., Gurney, J. J., and Richardson, S. H., 1985, Evidence for a 150-200-km thick Archean lithosphere

from diamond inclusion thermobarometry: Nature, v. 315, p. 387–409.

Campbell, I. H., and Griffiths, R. W., 1990, Implication of mantle plume structure for the evolution of fluid basalts: Earth and Planetary Science Letters, v. 99, p. 79–93.

Campbell, I. H., and Hill, R. I., 1988, A two-stage model for the formation of the granite-greenstone terrains of the Kalgoorlie-Norseman area, Western Australia: Earth and Planetary Science Letters, v. 90, p. 11–25.

Cogley, J.G., 1985, Hypsometry of the continents: Zietschrift für Geomorphologie, Supplementband 53.

Condie, K. C., 1998, Episodic continental growth and supercontinents: A mantle avalanche connection?: Earth and Planetary Science Letters, v. 163, p. 97–108.

Conrad, C. P., and Hager, B. H., 2001, Mantle convection with strong subduction zones: Geophysical Journal International, v. 144, p. 271–288.

Davies, D. G., 1986, Mantle convection under simulated plates: Effects of heating modes and ridge and trench migration, and implication for core-mantle boundary, bathymetry, geoid, and Benioff zone: Journal of the Royal Astronomical Society, v. 84, p. 153–183.

_____, 1988, Role of the lithosphere in mantle convection: Journal of Geophysical Research, v. 93, p. 10,451–10,466.

_____, 1989, Mantle convection model with a dynamic plate: Topography, heat flow, and gravity anomalies: Geophysical Journal International, v. 98, p. 461–464.

Doin, M.-P., Fleitout, L., and Christensen, U., 1997, Mantle convection and stability of depleted and undepleted continental lithosphere: Journal of Geophysical Research, v. 102, p. 2771–2787.

Fontigne, D., and Schilling, J. G., 1996, Mantle heterogeneities beneath the South Atlantic; a Nd-Sr-Pb isotopic study along the Mid-Atlantic Ridge (3°–46° S): Earth and Planetary Science Letters, v. 142, p. 209–221.

Forte, A. M., and Mitrovica, J. X., 2001, Deep-mantle high-viscous flow and thermochemical structure inferred from seismic and geodynamic data: Nature, v. 410, p. 1049–1056.

Gable, C. W., O'Connell, R. J., and Travis, B. J., 1991, Convection in three dimensions with surface plates: Generation of toroidal flow: Journal of Geophysical Research, v. 96, p. 8391–8405.

Grand, S. P., and Helmberger, D. V., 1984, Upper mantle structure beneath of North America: Geophysical Journal of the Royal Astronomical Society, v. 76, p. 399–438.

Gupta, M. L., 1993, Is the Indian Shield hotter than other Gondwana shields?: Earth and Planetary Science Letters, v. 115, p. 275–285.

Gurnis, M., 1988, Large-scale mantle convection and aggregation and dispersal of supercontinents: Nature, v. 332, p. 696–699.

Gurnis, M., and Hager, B. H., 1988, Control of the structure of subducted slab: Nature, v. 335, p. 317–321.

Gurnis, M., and Zhong, S., 1991, Generation of long wavelength heterogeneities in mantle dynamics: Interaction between plates and convection: Geophysical Research Letters, v. 18, p. 581–584.

Hanan, B. B., Blichert-Toft, J., Kingsley, R., and Schilling, J. G., 2000, Deplated Iceland mantle plume geochemical signature: Artifact of multicomponent mixing?: Geochemistry, Geophysics, and Geosystems, 1-2000, American Geophysical Union and the Geochemical Society, United States [paper number 1999GC000009].

Hill, R. I., Campbell, I. H., Davies, G. F., and Griffiths, R. W., 1992, Mantle plumes and continental tectonics: Science, v. 256, p. 186–193.

King, S. D., Gable, C. W., and Weinstein, S. A., 1992, Model of convection-driven tectonic plate: A comparison of methods and results: Geophysical Journal International, v. 109, p. 481–487.

Lenardic, A., 1997, On the heat flow variation from Archean cratons to Proterozoic mobile belts: Journal of Geophysical Research, v. 102, p. 709–721.

_____, 1998, On the partitioning of mantle heat loss below oceans and continents over time and its relationship to the Archean paradox: Geophysical Journal International, v. 134, p. 706–720.

Lenardic, A., and Kaula, W. M., 1995, Mantle dynamics and the heatflow into the Earth's continents: Nature, v. 378, p. 709–711.

Lowman, J. P., and Jarvis, J. T., 1993, Mantle convection flow reversal due to continental collisions: Geophysical Research Letters, v. 20, p. 2087–2090.

_____, 1995, Mantle convection models of continental collision and breakup incorporating finite thickness plates: Physics of the Earth and Planetary Interiors, v. 88, p. 53–68.

_____, 1996, Continental collisions in wide aspect ratio and high Rayleigh number: Two-dimensional mantle convection models: Journal of Geophysical Research, v. 101, p. 25,485–25,497.

_____, 1999, Effects of mantle heat source distribution on supercontinent stability: Journal of Geophysical Research, v. 104, p. 12,733–12,746.

Marzoli, A., Renne, P. R., Piccirillo, E. M., Ernesto, M., Bellieni, G., and De Min, A. 1999, Extensive 200-million-year-old continental flood basalts of the Central Atlantic Magmatic Province: Science, v. 284, p. 616–618.

Moresi, L.-N., and Lenardic, A., 1997, Three-dimensional numerical simulation of crustal deformation and subcontinental mantle convection: Earth and Planetary Science Letters, v. 150, p. 223–243.

Nisbet, E. G., 1987, The young Earth: An introduction to Archean geology: Boston, MA, Allen and Unwin, 402 p.

Olson, P., and Corcos, G. M., 1980, Boundary layer model for mantle convection with surface plates: Geophysical Journal of the Royal Astronomical Society, v. 62, p. 195–219.

Pearson, D. G., Shirey, S. B., Carlson, R. W., Boyd, F. R., Pokhilenko, N. P., and Shimuzu, N., 1995, Re-Os, Sm-Nd, and Rb-Sr isotopic evidence for thick Archean lithospheric mantle beneath the Siberian craton modified by multistage metasomatism: Geochimica et Cosmochimica Acta, v. 59, p. 959–977.

Pollack, H. N., Hurter, S. J., and Johnson, J. R., 1993, Heat flow from the Earth's interior: Analysis of the global data set: Reviews of Geophysics, v. 31, p. 267–280.

Richardson, S. H., Gurney, J. J., Erlank, A. J., and Harris, J. W., 1984, Origin of diamonds in old enriched mantle: Nature, v. 310, p. 198–202.

Samarskii, A. A., and Nikolaev, E. S., Methods of finite-difference equations solving: Moscow, Nauka Press, 1978, 591 p. (in Russian).

Schubert, G. Turcotte, D. L., and Olson, P., 2001, Mantle convection in the Earth and planets: Cambridge, UK, Cambridge University Press, 940 p.

Solomatov, V. S., and Moresi, L.-N., 2000, Scaling of time-dependent stagnant lid convection: Application to small-scale convection on Earth and other terrestrial planets: Journal of Geophysical Research, v. 105, p. 21,795–32,1817.

Stoddard, P. R., and Abbott, D. H., 1996, The influence of the tectosphere upon plate motion: Journal of Geophysical Research, v. 101, p. 5425–5433.

Tackley, P. J., 2000a, Self-consistent generation of tectonic plates in time-dependant, three-dimensional mantle convection simulations 1. Pseudoplastic yielding: Geochemistry, Geophysics, and Geosystems, v. 1 [paper number 2000G000036].

_____, 2000b, Self-consistent generation of tectonic plates in time-dependent, three-dimensional mantle convection simulations 2. Strain weakening and asthenosphere: Geochemistry, Geophysics, and Geosystems, v. 1 [paper number 2000GC000043].

Trubitsyn, V. P., 2000, Principles of the tectonics of floating continents: Izvestiya, Physics of the Solid Earth, v. 36, p. 101–113.

Trubitsyn, V. P., and Rykov, V. V., 1995, A 3-D numerical model of the Wilson cycle: Journal of Geodynamics, v. 20, p. 63–75.

_____, 1998, A self-consistent 2D model of mantle convection with a floating continent: Russian Journal of Earth Sciences, v. 1, p. 1–10 [http:\www.agu.org\wps\rjes].

_____, 2000, 3-D spherical models of mantle convection with floating continents: U.S. Geological Survey, Open File Report 00-218, 44 p.

Trubitsyn, V. P., Rykov, V. V., and Jacoby, W., 1999, A self-consistent 2-D model for the dip angle of mantle downflow beneath an overriding continent: Journal of Geodynamics, v. 28, p. 215–224.

Uyeda, S., 1982, Subduction zones: An introduction to comparative subductology: Tectonophysics, v. 81, p. 133–159.

Vail, R. M., and Mitchem, R. M., 1979, Global cycles of the relative changes of the sea level from seismic stratigraphy; in Watkins, J. S., Montadert, L., and Dickerson, P. W., eds., Geological and geophysical investigations of continental margins: American Association of Petroleum Geologists Memoir 29, Tulsa, OK.

VanDecar, J. C., James, D. E., and Assumpcao, M., 1995, Seismic evidence for a fossil mantle plume beneath South America and implications for plate driving forces: Nature, v. 378, p. 25–31.

White, R. S., and McKenzie, D., 1995, Mantle plumes and flood basalts: Journal of Geophysical Research, v. 100, p. 17,543–17,585.

Yu, Dongmei, Fontigne, D., and Schilling, J. G., 1997, Mantle-plume interactions in the central North Atlantic; a Nd isotope study of Mid-Atlantic Ridge basalts from 30 degrees N to 50 degrees N: Earth and Planetary Science Letters, v. 146, p. 259–272.

Zalesak, S.T., 1979, Fully multidimensional flux-corrected transport algorithms for fluids: Journal of Computers and Physics, v. 31, p. 335–361.

Zhong, S., and Gurnis, M., 1993, Dynamic feedback between a continent-like raft and thermal convection: Journal of Geophysical Research, v. 98, p. 12,219–12,232

_____, 1994, Role of plates and temperature-dependent viscosity in phase change dynamics: Journal of Geophysical Research, v. 99, p. 15,903–15,917.

_____, 1995, Mantle convection with plates and mobile, faulted plate margins: Science, v. 267, p. 838–843.

Zhong, S., Zuber, M. T., Moresi, L., and Gurnis, M., 2000, Role of temperature-dependent viscosity and surface plates in spherical shell models of mantle convection: Journal of Geophysical Research, v. 105, p. 11,063–11,082.

Appendix A

System of governing equations

Convection with moving rigid continents is described using the classical equations of mantle convection and Euler's equations for the motion of a body. The mantle is modeled by a liquid with variable viscosity and a phase transition. The rigid continent is assumed to be submerged in the convection mantle, like an iceberg in the ocean. Viscous drag of the convecting mantle moves the floating continent. The boundary conditions applied to the surfaces submerged in the mantle take into account all thermal and mechanical interactions with the viscous mantle. We are therefore able to compute both the velocity and heat flux of the continent. Our numerical code for mantle convection was verified by a benchmark comparison (Blankenbach et al., 1989). In order to assess numerical stability, we have compared results obtained with various grid spacings and Rayleigh numbers.

Equations of mantle convection

Thermal convection in a 2-D model is classically described by the Stokes equation, the equations of heat transfer, and the equation of continuity with variable parameters (c.f., Schubert et al., 2001):

$$-\partial p/\partial x + \partial[\eta(\partial V_x/\partial z + \partial V_z/\partial x)]/\partial z + 2\partial(\eta\partial V_x/\partial x)/\partial x = 0, \tag{1}$$

$$-\partial p/\partial z + \partial[\eta(\partial V_z/\partial x + \partial V_x/\partial z)]/\partial x + 2\partial(\eta\partial V_z/\partial z)/\partial z + Ra_0\, \alpha T = 0, \tag{2}$$

$$\partial T/\partial t + V_x\partial T/\partial x + V_z\partial T/\partial z = (\partial/\partial x)(\partial kT/\partial x) + (\partial/\partial z)(\partial kT/\partial z) + H, \tag{3}$$

$$\partial V_x/\partial x + \partial V_z/\partial_z = 0, \tag{4}$$

where V_x, and V_z, p, and T are dimensionless components of velocity, pressure, and temperature, respectively, and H is the internal heat production. As is customary, equaitons 1-4 are given in dimensionless form with the following parameters: D for distance; k_0 for the thermal conductivity; $\kappa_0 = k_0/\rho c_p$ for the thermal diffusivity; η_0 for the viscosity, κ_0/D for the velocity; T_0 for the temperature; D^2/κ_0 for the time; $\eta_0\kappa_0/D^2$ for the stresses; α_0 for the coefficient of thermal expansion; and c_{p0} for the thermal capacity. The Rayleigh number:

$$Ra = \alpha_0\rho g T_0\, D^3/ (\kappa_0\, \eta_0)$$

controls the intensity of mantle convection, where g is the acceleration due to gravity, and ρ is the density. Equations 1–3 can also be used to describe mantle phase transitions if we use generalized effective parameters α, c_p, and compressibility $1/K$, which include phase transitions with delta functions for the phase distribution (Schubert et al., 2001).

Equations of motion for the continents

We assume a continent to be a thick, perfectly rigid plate. In a 2-D model, the velocities of all points of the continents u (u_x, u_z) are equal to the velocity of the center of gravity for the plate u_x (x,z) = u_0, u_z (x,z) = 0.

A continent is propelled by the viscous forces of the mantle flow. The equation for its horizontal motion takes the form (Trubitsyn and Rykov, 1995; Trubitsyn et al. 1999):

$$m\partial u_0/\partial t =$$

$$\int_{1-d}^{1} [(p)_{x=x_1} - 2\eta(\partial V_x/\partial x)_{x=x_1}]dz -$$

$$\int_{1-d}^{1} [(p)_{x=x_2} - 2\eta(\partial V_x/\partial x)_{x=x_2}]dz - \tag{5}$$

$$\int_{x_1}^{x_2} \eta[(\partial V_x/\partial z)_{z=1-d} + (\partial V_z/\partial z)_{z=1-d}]dx,$$

where m is the dimensionless mass of the continental plate per unit length in the y-direction; d and l are the thickness and length of the continent, and $x_1(t)$ and $x_2(t) = x_1(t) + l$ are the instantaneous co-ordinates of its left and right edges, respectively, satisfying the condition:

$$dx_1/dt = u_0. \tag{6}$$

For slow convection in the mantle, the acceleration of a continent is very small and its motion is similar to mantle flow. The relation of the left side of eq. (5) to the right side is of order $k\rho/\eta_0 \sim 10^{-23}$. Therefore, the right side of eq. (5) can be set equal to zero, and the equation of motion of the continent is reduced to an integrated condition of force balances.

The equation for the temperature T_c (x, z) within the continent, in the basic co-ordinate system, includes the advective temperature with the velocity of the continent u_0 along the axis x:

$$\partial T_c/\partial t + u_0 \partial T_c/\partial x =$$
$$(\partial k_c/\partial x)(\partial T_c/\partial x) + (\partial k_c/\partial z)(\partial T_c/\partial z) + H_c, \quad (7)$$

where κ_0 is the thermal diffusivity for a continent, and Hc is its thermometric radioactive internal heat production.

Boundary conditions

We assume continuity for the temperature and the heat flow, and a no-slip boundary for the velocity $V_x = u_0$ and $V_z = 0$ on the submerged bottom and sides of the continent. As a result eq. 5 may be simplified (Trubitsyn et al. 1999) to:

$$\int_{1-d}^{1} [(p)_{x = x_1 + l} - (p)_{x = x_1}] dz + \quad (8)$$
$$\int_{x_1}^{x_1 + l} \eta(\partial V_x / \partial z)_{z = 1 - d} dx = 0.$$

Thus, the unknowns to be found in the mantle are the velocity components $V_x(x,z)$ and $V_z(x,z)$, pressure p(x,z), and temperature T(x,z). Other unknown variables to be solved for are the velocity $u_0(x)$ at the center of the rigid plate, the temperature within the continent $T_c(x,z)$ and the co-ordinate of its left edge $x_1(t)$. These seven unknown variables are found from the four equations of convection (1–4), coupled with the three equations of a moving plate (6–8). As these equations contain the large square-law terms $V_x \partial T/\partial x$, $V_z \partial T/\partial z$, and $u_0 \partial T_c/\partial x$, the system of the equations of mantle-continent is strongly nonlinear.

The set of equations (1–8) is solved by a finite-difference method based on flux-corrected transport algorithms (Zalesak, 1979) for tempera-ture transfer and alternating triangular matrix decomposition with iterative parameters obtained by the conjugate gradient method for velocities and pressure (Samarskiy and Nikolayev, 1978).

Calculation of elapsed time in numerical model

In order to partially remove the bias that is associated with a lower Rayleigh number, we have run our models for a long period of geological time. We have calculated the model time by extrapolating the calculated value of variables to Ra $\approx 10^7$. The Nusselt number, Nu, defines efficiency of heat transfer, and is the ratio of total heat flux to pure conductive heat flux. According to the boundary layer theory of mantle convection (Schubert et al., 2001) mantle velocity, V, is proportional to $Ra^{2/3}$ and Nu~$Ra^{1/3}$. Therefore, the typical time for mass transfer, τ_v, is proportional to $Ra^{-2/3}$. The typical time for heat transfer, τ_q, can be found from a dimensional analysis for equations of heat transfer and Nusselt number. Let us change all differentials in the equations $\partial T/\partial t = \kappa \partial^2 T/\partial z^2 - V_z \partial T/\partial z$ and $Nu = (V_z T - \kappa \partial T/\partial z)/(\kappa \Delta T/D)$ using finite differences $T/\tau_q = \kappa T/D2 - V_z T/D$ and $Nu = (V_z T - \kappa T/D)/(\kappa T/D)$.

By eliminating V_z, we find $\tau_q = D^2/(k\ Nu)$. As a result we have $\tau_v \sim Ra^{-2/3}$ and $\tau_q \sim Ra^{-1/3}$, or on average $\tau \sim Ra^{-1/2}$. Therefore to extrapolate the data, calculated for Ra $= 5 \cdot 10^4$, to the real Earth with Ra $= 10^7$, we need to use these extrapolated units for time $\tau = D^2/\kappa_0 (Ra/Ra_E)^{-1/2} = 3 \cdot 10^{11}$ y $\cdot (10^7/5 \cdot 10^4)^{-1/2} \approx 20$.

Besides horizontal motion of the continents, we also illustrate their uplift by hot, buoyant upwellings. Such dynamic topography of the free surface, which is in equilibrium with the convecting mantle, may be calculated using the relation:

$$h = (p - 2\ \eta \partial V/\partial z)/\rho g.$$

The maximum geoid anomaly is less than 100 m and the relief anomaly is on the order of 1 km.

Appendix B

The results presented in Figures 1–5 were calculated for a low Rayleigh number (Ra $= 2 \cdot 10^4$) in order to avoid the non-steady state and partially chaotic convection that occurs for higher Rayleigh numbers. To illustrate the effect of using a higher Rayleigh number (Ra), we present a numerical simulation for a moving continent of size 3000 km and $Ra_{ef} = 2 \cdot 10^6$, including effects of a phase boundary at a depth of 660 km and internal heating.

The blanketing effect of a stationary continent can reverse mantle flow from convective downwelling to upwelling in the time period τ~100-300 m.y. However, if the continent moves at a velocity greater than $D/\tau = 3 \cdot 10^8$ cm/10^8 yr = 3 cm/yr, where
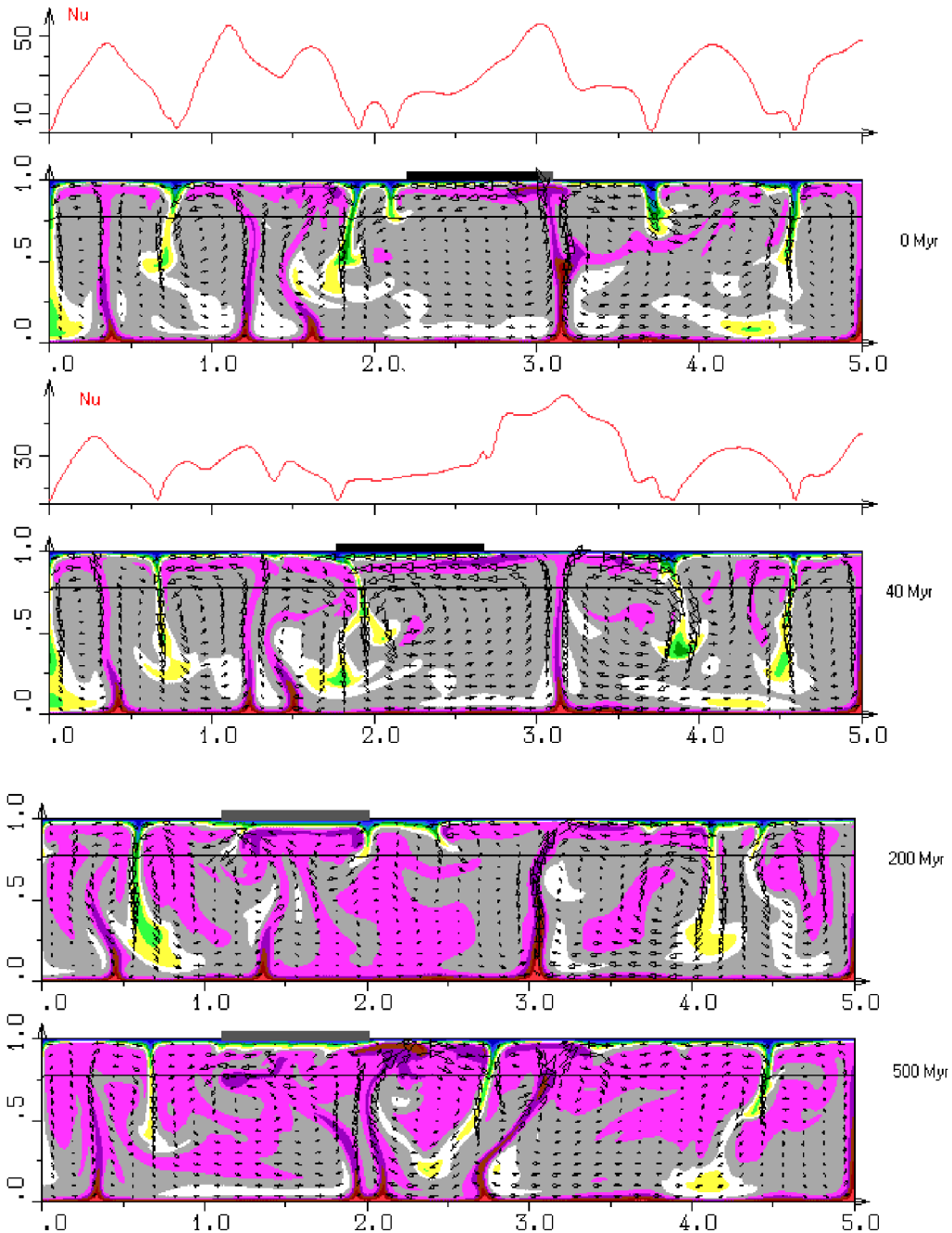
FIG. B1. Evolution of mantle convection with the presence of a single large continent ($l = 3000$ km) and for $Ra_{ef} = 2 \cdot 10^6$. The model is both basally and internally heated and includes a phase boundary at 660 km. Note that the convection pattern is much more chaotic than in Figures 1–5. The color scale for dimensionless temperature is the same as that used in Figure 1. At times $t_1 = 0$ and $t_2 = 40$ m.y., the continent is free floating. At times $t_3 = 200$ m.y. and $t_4 = 500$ m.y., the continent is restrained from moving. As expected, the continent moves away from the strong upwelling at $x = 3.1$. However, due to the higher Rayleigh number and more complex convection pattern, it is more difficult to isolate the long-wavelength effect of the continent on the system. For this reason, we have used a lower Rayleigh number in the simulations of Figures 1–5.

D is the thickness of the mantle, the mantle has insufficient time to heat up and there is no blanketing effect. We demonstrate this important observation with a model of mantle convection with a superadiabatic Rayleigh number $Ra_{ef} = 2 \cdot 10^6$ and internal heating $H = 20$ (which corresponds about half heating from below and half inside). Also we take into account the phase transition at 660 km,

which is the most significant phase transition for mantle convection. The Claperon slope of the phase transition was taken as $\gamma l = dp/dT = -2$ MPa/K and a density jump of $\Delta\rho/\rho = 0.09$ was assumed at the phase transition.

The calculations were done for an elongated 2-D box with an aspect ratio of 5:1, and with a grid of 400×150 and 400×300, which corresponds to space steps $\Delta x = 0.0125 = 37.5$ km and $\Delta z = 0.00667 = 20$ km or 10 km, respectively. The dimensionless viscosity was taken as a function of the super-adiabatic temperature and hydrostatic pressure in the form $\eta(T, p) = 5.0 \cdot \exp[-6.9\,T + 4.6(1 - z)]$.

Due to the temperature increase from the top to the bottom of the mantle, viscosity decreases by three orders of magnitude. However, the pressure change between the top and bottom of the mantle increases viscosity by two orders of magnitude. The mean logarithm of dimensionless viscosity is equal to about 1. The thickness of the continent was taken as $d = 0.0333 = 100$ km and the length as $l = 0.9 = 2700$ km.

Figure B1 (t = 0 m.y.) shows the state of mantle convection at the exact moment when the continent was instantaneously introduced into the mantle. Note that the mantle convection is non-steady state. Downwellings (green) and upwellings (pink) penetrate through the phase boundary, but often change their form as they pass through the boundary. For example, a downwelling at x = 0.7 splits at the phase boundary and a downwelling at x = 3.7 becomes wider at the phase boundary. The upwelling at x = 1.2 bends to the left, and the upwelling at x = 3.2 branches horizontally before reaching the phase boundary at z = 0.5. Due to viscous drag, the continent moves to the left. At t = 40 m.y. it has moved $\Delta x \approx 400$ km with a mean velocity $V \approx 1$ cm/y. This velocity is about 5–7 times less than the mantle velocity. It can be explained by the hindering effect of the subduction zone in front of the continent. The simulation at t = 40 m.y. shows the situation when the left corner of the continent encounters a downwelling and disturbs the geometry of the uppermost limb of this downwelling. As a result, the downwelling slopes under the continent, much like a subducting plate. This stage of the mantle-continent system mimics the present state of the South American continent. The blanketing effect has not yet appeared.

At time t = 200 m.y. the continent has slowly moved further to the left, and we have stopped the continent from moving. This lack of motion induces the blanketing effect, and the mantle under the continent becomes warmer. As a result, the pressure in the mantle under the continent becomes lower. The low pressure is sufficient to pull upwellings along the core-mantle boundary. At time t = 500 m.y. the strong upwelling that was at x = 3.0 at time t = 200 m.y. has shifted to x = 2.0 and an additional weaker upwelling has appeared at x = 2.6.

This simulation emphasizes the more chaotic convection for higher Rayleigh numbers, and illustrates the blanketing effect of a near-motionless continent, such as present-day Africa. See also Trubitsyn and Rykov (1998).